Viscosity Dependence of the Local Segmental Dynamics of Anthracene-Labeled 1,2-Polybutadiene in Dilute Solution

S. Adams and D. B. Adolf*

Department of Physics and Astronomy, University of Leeds, Leeds LS2 9JT, U.K.

Received March 11, 1998; Revised Manuscript Received June 5, 1998

ABSTRACT: Time-correlated single-photon-counting measurements have been performed on anthracene-labeled 1,2-polybutadiene. The local segmental dynamics were observed in seven solvents covering a viscosity range of more than three decades and over the temperature range of 280−350 K. Correlation times were extracted from the fluorescence anisotropy decays and were determined as a function of temperature in all solvents. The observed temperature and viscosity dependence has been examined in terms of Kramers' theory in the high friction limit and two empirical equations, those of Fleming and co-workers and Robinson, both of which incorporate the idea of frequency-dependent friction developed by Grote−Hynes. It was found that the dynamics scaled as the viscosity to the power 0.82 ± 0.04.

Introduction

Comparisons between local polymer motion on the length scale of a few repeat units and longer length scale polymer dynamics offer valuable insight into the influence of atomistic detail on macroscopic polymer properties. Whereas the most direct connection is made in the bulk state, monitoring these short-length-scale motions in dilute solution offers the opportunity to investigate intrachain dynamics in the absence of interchain interactions.

Time-correlated single-photon-counting measurements of anthracene-labeled 1,2-polybutadiene (1,2PB) have been performed in seven solvents over the temperature range 280−350 K. This utilized the viscosity range 0.3−1500 cP. The current results are compared to those of a recent ^{2}H NMR investigation of 1,2PB.[1] Kramers' theory, in the high friction limit and in the absence of specific polymer/solvent interactions, predicts that the local dynamics will scale linearly with the solvent viscosity. Both the current optical experiments and the ^{2}H NMR experiments demonstrate a failure of Kramers' theory. The incorporation of a frequency-dependent friction is required to fit the data. In both the optical and NMR cases, the local dynamics show a power law dependence on the viscosity. The value of the exponent reported here, 0.82 ± 0.04, differs significantly from the value reported in the ^{2}H NMR experiments, 0.43. Such differences between optical and NMR experiments have been noted before when comparing optical[2] and NMR[3] measurements of *cis*-1,4-polyisoprene.

Method

Materials and Sample Preparation. The polybutadiene chains used in this study were provided by Polymer Laboratories. They contain one anthracene chromophore covalently bonded in the middle of the chain (see Figure 1). The $S_0 \rightarrow S_1$ electronic transition dipole moment, the double-headed arrow of Figure 1, of the anthracene chromophore is oriented along the chain backbone, and hence any movement of the dipole reflects movement of the polymer backbone. The samples employed had $M_w = 67\,000$ and a polydispersity of 1.19. The chain microstructure was 86% vinyl 1,2 units and 14% 1,4 units.

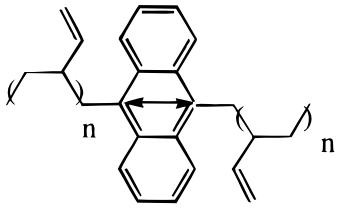

Figure 1. Structure of anthracene-labeled 1,2-polybutadiene. The $S_0 \rightarrow S_1$ transition is indicated by the double-headed arrow.

Solutions of 1,2PB were prepared in seven solvents: toluene, cyclohexane, *n*-dodecane, decalin, squalane, dioctyl phthalate, and Arochlor 1248. Toluene, cyclohexane, *n*-dodecane, squalane, and dioctyl phthalate all were used as received (Aldrich; all ≥99% purity). Decalin was used as received (Aldrich) at 98% purity. Arochlor (Greyhound Chemicals), a mixture of polychlorinated biphenols, 48% chlorine by weight, was used as received. The viscosities of the solvents are reported in the literature[3−5] over the temperature range utilized here. The Arrhenius activation energies have been reported by Adolf et al.[2] The optical densities of the polymer solutions at 406 nm were in the range 0.05−0.1 in a 3 mm path length cuvette, corresponding to a concentration of ≤0.5 wt %. Solutions were filtered (0.45 μm) and subjected to several freeze−pump−thaw processes to replace the molecular oxygen with molecular nitrogen.

Experimental Technique. Fluorescence anisotropy decay data were collected using the method of time-correlated single photon counting.[6] A schematic of the experimental apparatus is shown in Figure 2. A frequency-doubled, mode-locked Nd:YAG laser pumped a styryl 9 dye laser. The 4 MHz cavity-dumped output gave linearly polarized picosecond pulses at 812 nm, which was frequency-doubled to produce the 406 nm excitation pulses. The excitation beam was then split, and ∼4% was detected by a fast photodiode which triggered off the remaining undoubled light. The signal from this was sent through a constant fraction discriminator (CFD) to the time to amplitude converter (TAC). The remainder of the light was passed through a filter to remove any undoubled light and a Fresnel Rhomb to select the vertical polarization before the train of pulses passed through to the sample. The fluorescence from the sample was collected and focused through a polarizer into a 1 nm band-pass monochromator set at 414 nm. The output from the monochromator was detected by a multichan-

* To whom correspondence should be addressed. Telephone: 0113 2333812. Fax: 0113 2333846.

S0024-9297(98)00386-6 CCC: $15.00 © 1998 American Chemical Society
Published on Web 08/01/1998

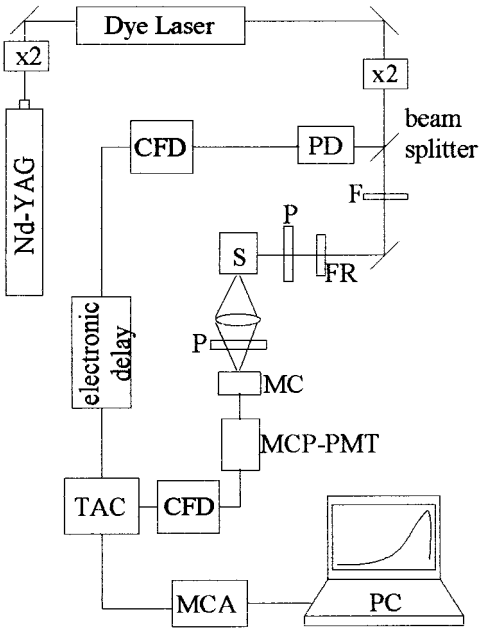

Figure 2. Schematic of the time-correlated single-photon-counting apparatus: MCP-PMT, microchannel plate photomultiplier tube; PD, photodiode; CFD, constant fraction discriminator; TAC, time to amplitude converter; MCA, multichannel analyzer; MC, monochromator; ×2, frequency-doubling crystal; P, polarizer; FR, Fresnel Romb; F, filter; S, sample; PC, personal computer.

nel plate photomultiplier tube (MCP-PMT, Hamamatsu R3809U). The signal was amplified and sent through a second CFD to the TAC operating in reverse mode. The data were stored on a personal computer. Time-correlated single photon counting relies on the premise that the probablility distribution for the emission of a single photon is equivalent to the real-time fluorescence decay of the sample. The fluorescence count rate was kept at ≤0.5% of the excitation rate to prevent pulse pileup. A ground-glass plate was used to measure the instrument response function, which had a fwhm of ∼60 ps for all experiments reported here. This was iteratively deconvolved from the data before analysis.

The frequency-doubled polarized pulse from the dye laser was used to photoselect an anisotropic distribution of anthracene chromophores. These chromophores emit light polarized along the $S_0 \rightarrow S_1$ transition dipole moment; hence, the emission from the sample was initially partially polarized. Molecular motions of the polymer backbone randomize the orientation of the excited-state chromophores and depolarize the emission. The reorientation of the transition dipole can be observed by monitoring the components of the fluorescence decay polarized parallel ($I_{\parallel}(t)$) and perpendicular ($I_{\perp}(t)$) to the excitation radiation. The time-dependent anisotropy $r(t)$ is constructed from the measured decays as

$$r(t) = \frac{I_{\parallel}(t) - I_{\perp}(t)}{I_{\parallel}(t) + 2I_{\perp}(t)} \tag{1}$$

This describes the time dependence of the reorientation of the excited-state chromophores and is directly related to a second-order orientation autocorrelation function, CF(t),

$$r(t) = r_0 \mathrm{CF}(t) \tag{2}$$

which describes the average reorientation of the transition dipole between the times of excitation and emission through

$$\mathrm{CF}(t) = \langle P_2(\cos\theta(t)) \rangle \tag{3}$$

P_2 is the second Legendre polynomial, and $\theta(t)$ is the angle through which a transition dipole moment has rotated in a time t since the excitation pulse. The angular brackets indicate an ensemble average over all the excited-state transition dipole moments. Thus, the observation of $I_{\parallel}(t)$ and $I_{\perp}(t)$ allows the direct calculation of the orientation autocorrelation function without the assumption of any motional model.

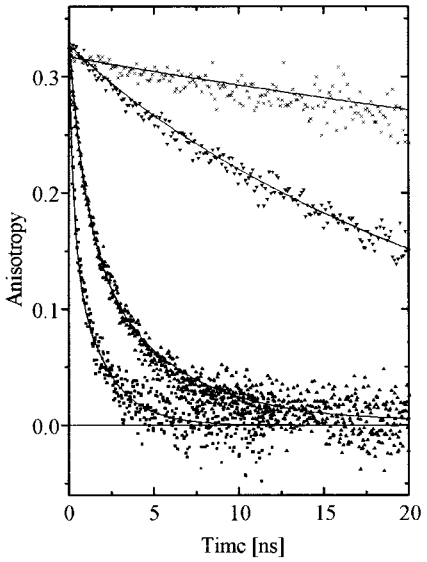

Figure 3. Representative anisotropy decays for 1,2-polybutadiene dynamics at 20 °C in dilute solution with, from top to bottom, arochlor, squalane, dodecane, and toluene. The dots are experimental data, and the lines are best fits to the biexponential model.

Data Analysis. The anisotropy decays were fit to an empirical biexponential function

$$r(t) = A \exp\{t/\tau_1\} + B \exp\{t/\tau_2\} \tag{4}$$

The quantities A, B, τ_1, and τ_2 are the fitting parameters. These fits are only meant to convey the shape of the anisotropy decay, and no physical significance is attributed to these parameters. The sum $A + B$ is equated to r_0 of eq 2. This parameter is related to the angle between the absorption and emission dipoles in the chromophore and should be constant for a given chromophore. The average value obtained in the current work was 0.33 ± 0.04 over all temperatures and viscosities. This is in good agreement with previous studies of other anthracene-labeled polymers.[2,7] Fits to this model typically gave reduced χ^2 values of ≤1.2. The correlation time, τ_c, was used to characterize the anisotropy decays as

$$\tau_c = \int_0^\infty \mathrm{CF}(t)\, \mathrm{d}t \tag{5}$$

In terms of the biexponential model used here

$$\tau_c = \frac{A\tau_1 + B\tau_2}{A + B} \tag{6}$$

We estimate the error in the reported τ_c values to be ±15%.

Results and Discussion

Figure 3 shows the anisotropy decay from the anthracene-labeled 1,2PB in four of the seven solvents (arochlor, squalane, dodecane, and toluene from top to bottom) at 20 °C. The decays shown have correlation times ranging from 986 ps (bottom) to 236 ns (top). The correlation times for the local dynamics in all seven solvents over the temperature range 280−350 K are plotted in Arrhenius format in Figure 4. The observed correlation times cover approximately three decades in time. As expected, the slowest dynamics occur in Arochlor 1248, the most viscous solvent and the fastest

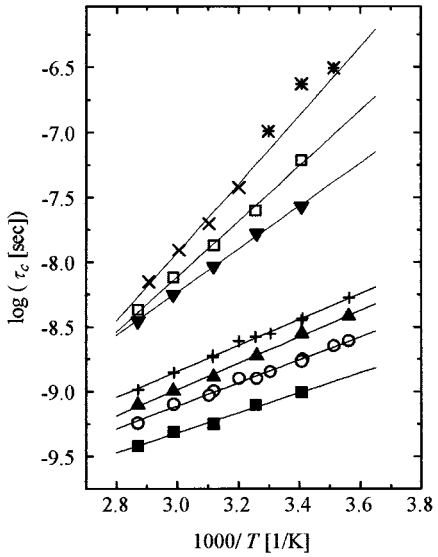

Figure 4. Correlation times for the dilute solution local dynamics of anthracene-labeled 1,2-polybutadiene plotted in Arrhenius format. The solvents are toluene (■), cyclohexane (○), *n*-dodecane (▲), decalin (+), squalane (▼), dioctyl phthalate (□), and Arochlor 1248 (× and *). The stars represent experiments where only a small fraction of the anisotropy decay was seen within the experimental time window. These values were not used in the later analysis. The slope of each solid best fit line for each solvent is related to the experimental activation energy for 1,2-polybutadiene local dynamics in that solvent.

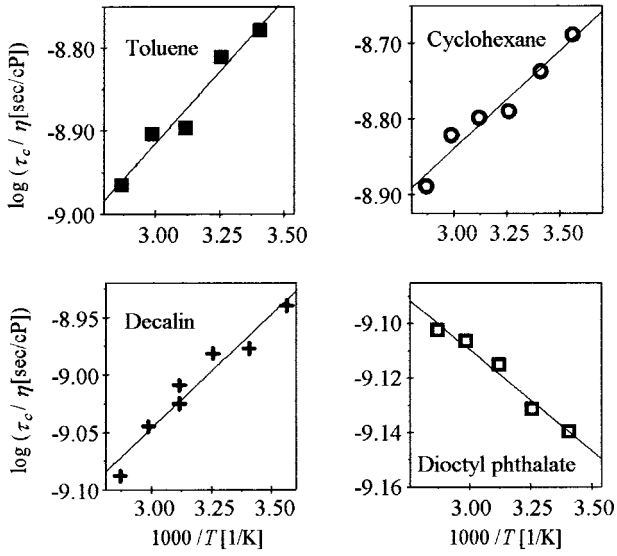

Figure 5. Test of Kramers' theory. The negative slope of dioctyl phthalate demonstrates that Kramers' theory is inadequate in the high friction limit. The symbols are the same as those for Figure 4.

in toluene, the least viscous solvent. The activation energy for 1,2PB local dynamics within each solvent can be calculated from the slope of each line of best fit in Figure 4.

Kramers' Theory. Kramers' theory, in the high friction limit and in the absence of any specific solvent/polymer interactions, predicts that the correlation time will scale linearly with solvent viscosity,[8] η.

$$\tau_c = A\eta \exp\{E_a/RT\} \tag{7}$$

It is unlikely that the assumptions made are inconsistent with the current experiment as has been discussed previously.[1,2] The failure of Kramers' theory can be demonstrated by plotting $\log(\tau_c/\eta)$ against $1000/T$. Such plots have been constructed for four of the solvents used and are shown in Figure 5. The activation energies found from these plots are 7, 5, 4, and −1 kJ mol^{-1}. A negative activation energy is nonphysical and clearly demonstrates that Kramers' theory is not adequate to describe the current data.

Grote−Hynes Theory. Grote and Hynes generalized Kramers' theory by allowing the friction opposing the local polymer motions to be frequency dependent when the solvent motions and the polymer motions do not occur on widely separated time scales.[9] In such a regime, many of the low-frequency solvent motions, which contribute to the zero-shear viscosity, will be too slow to have any influence on the fast polymer motions.

Fleming and co-workers[10] proposed eq 8 as an empirical power law dependence of the local dynamics on the solvent viscosity. A plot of $\log(\tau_c)$ vs $\log(\eta)$ at 350 K is

$$\tau_c = A'\eta^{\alpha} \exp\{E_a/RT\} \tag{8}$$

shown in Figure 6. The best fit to the data of Figure 6 (the solid line) gives an α value of 0.82 ± 0.02. Similar plots have been constructed at several temperatures;

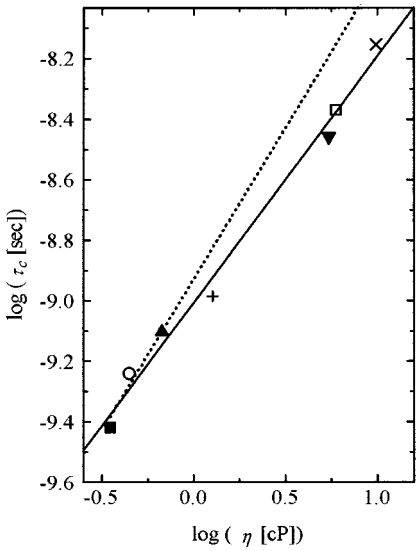

Figure 6. τ_c at 350 K as a function of solvent viscosity. The solid line is the best fit through the data and has a slope of 0.82. The dotted line has a slope of 1.0. The symbols are the same as those for Figure 4.

the slopes of these lines all lie within the range 0.82 ± 0.04. Equation 7 would predict a linear scaling with solvent viscosity, η. The dotted line of Figure 6 has a slope of 1; the deviation of the data from this line is a further demonstration of the failure of Kramers' theory.

One consequence of eq 8, if one assumes an Arrhenius form for the temperature dependence of the steady shear viscosity of the solvent, is

$$E_{exp} = E_a + \alpha E_\eta \tag{9}$$

E_{exp} is the experimentally observed activation energy (taken from each of the slopes in Figure 4), E_a is the activation energy for the local polymer motion, and E_η is the Arrhenius activation energy of each solvent's viscosity.[2] It is noted that the temperature dependence of the highest viscosity solvents is not strictly Arrhenius, so E_η only approximates to the true temperature dependence. Plotting E_{exp} against E_η gives a value for α

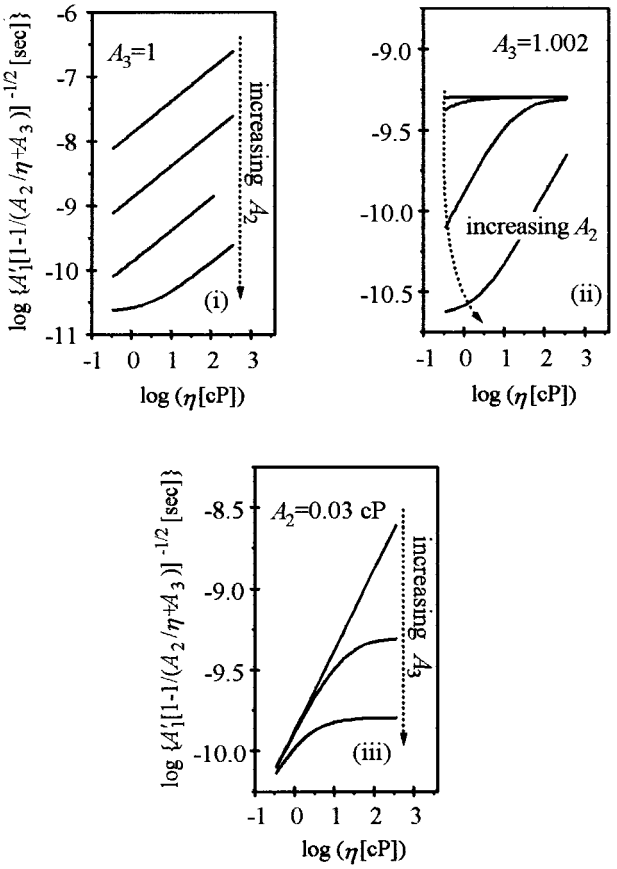

Figure 7. Plots of data generated from the Robinson equation, $\log\{A_1'[1 - 1/(A_2/\eta + A_3]^{-1/2}\}$, against $\log(\eta)$, to demonstrate the functional form of the Robinson equation. Graphs i and ii show the changing shape as parameter A_2 is varied. A_2 values from top to bottom are 0.000 003, 0.0003, 0.03, and 3. Graph iii shows the influence of A_3. Values of A_3, from top to bottom, are 1, 1.002, and 1.02.

of 0.80 ± 0.03 and an activation energy, E_a, of 8 ± 2 kJ mol^{-1}. This plot is not shown.

Robinson Equation. Robinson and co-workers have proposed a different functional form for the viscosity dependence of reaction rates,[11] giving rise to an expression for the correlation time as a function of viscosity:

$$\tau_c = A_1'\left[1 - \frac{1}{\{A_2/\eta\} + A_3}\right]^{-1/2} \exp\{E_a/RT\} \quad (10)$$

The equation was developed to describe the isomerization processes of small molecules, such as stilbenes in solution. The model has been applied successfully to both experiment and molecular dynamics simulations of small-molecule motions. This model has also been previously applied to the local polymer dynamics of an anthracene-labeled polystyrene by Ono et al.[12] The ranges of values reported for parameters A_2 and A_3 are 0−8.7 cP^{-1} and 1−1.1, respectively. A_1' is a scaling factor on the order of the time scale for the dynamics, 10^{-12}−10^{-11} s. An attempt was made to fit the current data to this equation with no success. To understand this better, it was decided to examine the functional form of the Robinson equation more closely.

Figure 7 shows plots of data generated from the Robinson equation in the form $\log\{A_1'[1 - 1/\{(A_2/\eta) + A_3\}]^{-1/2}\}$ vs $\log(\eta)$ over the viscosity and temperature ranges used within this investigation. Plots are shown for various values of the parameters A_2 and A_3 from eq 10. Only the shape of the Robinson equation is considered here so the scaling factor A_1' is constant in all cases at 2×10^{-11} s.

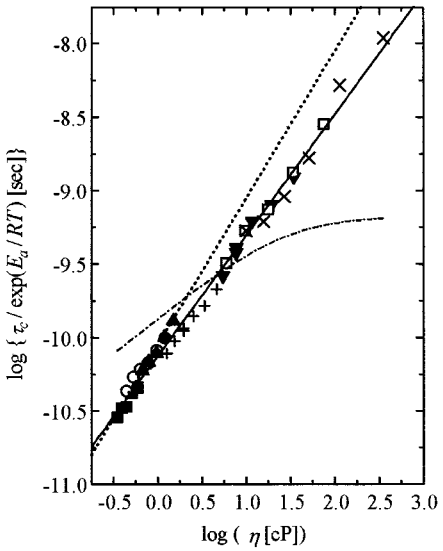

Figure 8. Master plot based on eq 8. The solid line is the line of best fit which gives an α value, from eq 8, of 0.82. The dotted line respresent Kramers' theory in the high friction limit, and the dot−dashed line is a plot of the Robinson equation with $A_2 = 0.03$ and $A_3 = 1.001$. The solvent symbols are the same as those for Figure 4.

It is observed that when $A_3 = 1$ and η is very much greater than A_2, the Robinson equation reduces to a form similar to eq 8 with $\alpha = {}^1/_2$. This can be seen in graph i of Figure 7, where all lines are parallel with a slope equal to $^1/_2$. Only when A_2 becomes very high relative to the viscosity (the lowest curve of graph i) does the Robinson equation show any curvature over the current range of viscosities. Graph ii illustrates how A_2 affects the shape of the curve with A_3 set equal to 1.002. It can be seen that even a slight increase in A_3, from 1 to 1.002, gives rise to very different behavior. With $A_3 > 1$, the Robinson equation predicts saturation. This leveling off of the correlation times at high viscosity is not seen in the current work. As A_3 is increased still further, the saturation point moves to lower viscosities (graph iii of Figure 7). The form of the Robinson equation over a large viscosity range is an "s"-shaped curve. The asymptotic behavior to zero gradient at low viscosities is controlled by the ratio of A_2 to the viscosity η. The position of the point of inflection and the high viscosity plateau are controlled by A_3. The maximum gradient at any region of this "s" curve will be 0.5. This is clearly not consistent with an α value of 0.82.

A master plot of all the data is presented in Figure 8 in the form $\log\{\tau_c/\exp(E_a/RT)\}$ vs $\log(\eta)$. The temperature dependence of the dynamics has been removed by dividing through by $\exp(E_a/RT)$, where E_a is taken to be 8 kJ mol^{-1} as found in the Fleming analysis. The data fit a straight line reasonably well, with the line of best fit (the solid line) having a slope of 0.82 ± 0.06. This demonstrates that the data fit eq 8 to a good approximation. A similar plot of $\log(\tau_c/\eta^{0.82})$ against $1000/T$ affords an activation energy of 7.8 ± 2 kJ mol^{-1} in close agreement with the results from eq 9. This plot is not shown. The dotted line of Figure 8 describes Kramers' theory in the high friction limit where $\alpha = 1.0$. The local dynamics clearly show a weaker dependence on the solvent viscosity than is predicted by

Table 1. Comparison of Viscosity Exponents and Activation Energies of Optical and NMR Measurements for Various Polymers

polymer	technique	α	E_a [kJ mol^{-1}]	viscosity range [cP]	temp range [K]	dynamic range [ns]	T_g[a] [K]	reference
1,2PB	optical	0.82 ± 0.04	8 ± 2	0.3−1600	280−350	0.4−300	245−283	this work
	NMR	0.43	14 ± 3	0.3−3	315−415	0.04−0.15		1
PI	optical	0.75 ± 0.06	10 ± 1	0.4−30 000	270−340	0.3−800	200	2
	NMR	0.41 ± 0.02	13 ± 2	0.3−30	250−360	0.015−0.16		3
PS	optical	0.9 ± 0.05	11 ± 3	0.3−35	270−360	1.2−200	373	7
	NMR	0.76 ± 0.05	14 ± 3	0.3−4	300−420	0.15−0.75		13

[a] Values of T_g are approximate values given only as a guide, taken from ref 15.

Kramers' theory. The dot−dashed line of Figure 8 is a plot of the Robinson equation using reasonable parameters of $A_2 = 0.03$ and $A_3 = 1.001$. It is clear from this that the Robinson equation fails to capture even qualitatively the viscosity dependence of the current data.

Comparison with Other Work

Zhu and Ediger studied the local dynamics of a per deuterated 1,2-polybutadiene in five solvents as a function of temperature.[1] They also found that their results were consistent with eq 8, although with parameters of $E_a = 14 \pm 3$ kJ mol^{-1} and $\alpha = 0.43$, in comparison with those of $E_a = 8 \pm 2$ kJ mol^{-1} and $\alpha = 0.82 \pm 0.04$ in the current optical study. Differences between optical and NMR parameters have been noted before in a comparison between ^{13}C NMR[3] and optical[2] experiments using *cis*-1,4-polyisoprene (PI). More recently, a more extensive NMR investigation of the dilute solution dynamics of polystyrene (PS)[13] has enabled yet another comparison to be made between this and previous optical studies.[7] These studies used eq 8 to analyze the viscosity dependence of the data. The results of each of the experiments are given in Table 1. For a given polymer, the α values obtained from the NMR experiments are smaller than the corresponding α values derived from the optical experiments. This behavior is consistent with the observation that motions probed by the optical technique are slower than those probed by NMR for a given polymer in the same solvent at the same temperature. The slower dynamics imply a larger separation of motional time scales between the polymer and solvent dynamics, thereby affording Kramers-like behavior with $\alpha \rightarrow 1$. α is known to depend on the size, shape, and mass of the isomerizing unit. Larger units favor values closer to 1. This also is consistent with the data in Table 1 since the relevant unit for the optical experiment incorporates an anthracene chromophore in contrast to the NMR measurements which sense the motion of a C−D bond vector.

The observed optical E_a values are consistently lower than those determined by NMR, with the largest difference being associated with 1,2PB. This behavior is due in large part to the value of 8 kJ mol^{-1} determined in this study. This seems low in comparison to the expected barrier height for polyethylene (12 kJ mol^{-1}),[15] which has the same chain backbone. To determine whether 8 kJ mol^{-1} is a reasonable barrier height for unlabeled 1,2PB local dynamics, molecular mechanics calculations were performed on molecules resembling portions of a 1,2PB backbone using MSI molecular modeling software and the polymer consortium force field.[16] 3-Ethyl-5-methylhepta-1,6-diene represents the head to tail addition of two 1,2PB monomers, 3,4-diethylhexa-1,5-diene the head to head addition, and 3,6-dimethylocta-1,7-diene the tail to tail addition of two such monomers. Each backbone dihedral angle of each

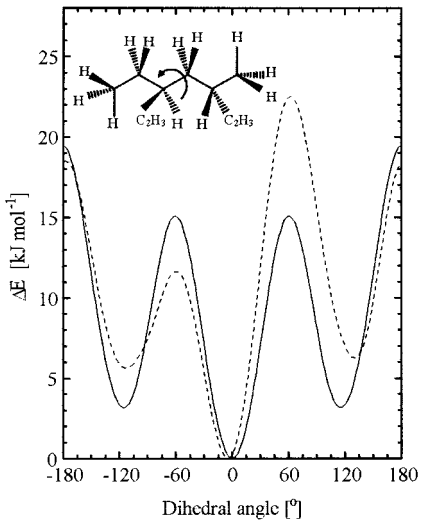

Figure 9. Molecular mechanics energy (ΔE) at various values of dihedral angle. 3-Ethyl-5-methylhepta-1,6-diene (C_2H_3 denotes a vinyl side group), the dashed curve, resembles a portion of a 1,2-polybutadiene chain. The dihedral angle used in the above calculation is illustrated in the inset with the angle at 0°. The solid line shows the calculation for hexane, used to represent polyethylene.

molecule was fixed at angles ranging from 0° to 360°, while the intramolecular energy of the remaining portion of the molecule was minimized. Typical findings are shown by the dashed line in Figure 9 for the molecule and dihedral angle indicated in the inset. The figure also presents results for the same dihedral angle in hexane (solid line) used to resemble a portion of a polyethylene chain. Both curves have three wells, but the dashed line does not possess the same symmetry about 0° as the solid line, apparently due to the presence of the vinyl side groups. The peaks at ∼ 60° and the valleys at ∼±120° for the dashed line lie above those of the solid line. However, the peak for the dashed line at −60° lies *beneath* the solid line, yielding an activation energy from the −120° state to the 0° state of ∼ 4 kJ mol^{-1}. A similar analysis for the backbone dihedral angles for the other molecules resembling portions of a 1,2PB backbone revealed barrier heights ranging from 4 to 23 kJ mol^{-1}. Therefore, a barrier height of 8 kJ mol^{-1} apparently is reasonable if one considers a typical 1,2PB chain to have barrier heights that span this range.

Conclusions

Fluorescence anisotropy decay with time-correlated single photon counting has been used to study the local dynamics of anthracene-labeled 1,2-polybutadiene as a function of temperature in a range of solvents spanning more than three decades in viscosity. Grote−Hynes theory adequately describes the data. The correlation time was found to scale with solvent viscosity as $\tau_c \propto$

$\eta^{0.82\pm0.04}$. The results from a recent ^{2}H NMR study were also found to follow this form but with a smaller exponent. These results are consistent with polymer and solvent motions occurring on similar time scales. The experimentally determined activation energy of 8 $\pm$ 2 kJ mol^{-1} is reasonable in light of molecular mechanics calculations.

Acknowledgment. We are indebted to Dr. T. Nicholson for the molecular mechanics work on the butadiene dimers. Financial support from EPSRC is gratefully acknowledged.

References and Notes

(1) Zhu, W.; Ediger, M. D. *Macromolecules* **1995**, *28*, 7549.
(2) Adolf, D. B.; Ediger, M. D.; Kitano, T.; Ito, K. *Macromolecules* **1992**, *25*, 867.
(3) Glowinkowski, S.; Gisser, D. J.; Ediger, M. D. *Macromolecules* **1990**, *23*, 3520.
(4) Viswanath, D. S.; Natarajan, G. *Data Book on the Viscosity of Liquids*; Hemisphere Publishing: New York, 1989.
(5) Barlow, A. J.; Lamb, J.; Matheson, A. J. *Proc. R. Soc. London A* **1966**, *292*, 322.
(6) O'Conner, D. V.; Phillips, D. *Time-correlated Single Photon Counting*; Academic Press: New York, 1984.
(7) Waldow, D. A.; Ediger, M. D.; Yamaguchi, Y.; Matsushita, Y.; Noda, I. *Macromolecules* **1991**, *24*, 3147.
(8) Kramers, H. A. *Physica* **1940**, *7*, 284.
(9) Grote, R. F.; Hynes, J. T. *J. Chem. Phys.* **1980**, *73*, 2715.
(10) Velsko, S. P.; Waldeck, D. H.; Fleming, G. R. *J. Chem. Phys.* **1983**, *78*, 249.
(11) Lee, J.; Zhu, S.-B.; Robinson, G. W. *J. Phys. Chem.* **1987**, *91*, 4273.
(12) Ono, K.; Okada, Y.; Yokotsuka, S.; Ito, S.; Yamamoto, M. *Polym. J.* **1994**, *26*, 199.
(13) Zhu, W.; Ediger, M. D. *Macromolecules* **1997**, *30*, 1205.
(14) Brandrup, J.; Immergut, E. H. *Polymer Handbook*, 2nd ed.; John Wiley and Sons: London, 1975.
(15) Ryckaert, J. P.; Bellemans, A. *Chem. Phys. Lett.* **1975**, *30*, 123. Steele, D. J. *J. Chem. Soc., Faraday Trans. 2* **1985**, *81*, 1077.
(16) Computational results obtained using software programs from Molecular Simulations − models built using Insight 3.0.0 and simulations performed by Discover 95.0 using the Polymer Consortium Force Field version 3.0.0.

MA980386M